QUARKS: Brazilian Electronic Journal of Physics, Chemistry and Material Science
journal homepage:
https://periodicos.ufjf.br/index.php/quarks
e-ISSN: 2674-9688

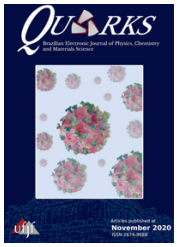

On the influence of low silica content on phosphates glasses doped with Erbium Ions

Diogo Rúbio Sant'Anna das Dores[a], Victor Rocha[a], Geraldo H. Silva[c], Victor H. de Oliveira[a], Zélia M. Da Costa Ludwig[a,*], Maria J. V. Bell[a], Valdemir Ludwig[a], Walter M. Pontuschka[b,*], Virgílio Anjos[a]

[a] *Universidade Federal de Juiz de Fora, Departamento de Física, CP 36036-330, Juiz de Fora- MG, Brazil*
[b] *Instituto de Física da Universidade de São Paulo, 05508-090 Cidade Universitária, São Paulo, São Paulo Brazil*
[c] *Instituto Federal de Educação, Ciência e Tecnologia do Rio de Janeiro (IFRJ) - Campus Pinheiral, Rio de Janeiro, Brazil*

Article history: Received: August 2020; Revised: September 2020; Accepted: October 2020. Available online: November 2020.
https://doi.org/10.34019/2674-9688.2020.v3.30205

Abstract

This work describes the spectroscopic characterization of a phosphate glass matrix doped with different Erbium concentrations. In order to increase the resistance of the glass, 3 mol % of silicon oxide were added to the phosphate matrix. A study of the optical absorption, luminescence and lifetime was conducted in order to characterize the infrared emission of Er^{3+} ions at 1540 nm, due to the radiative transition $^4I_{13/2} \rightarrow {}^4I_{15/2}$. Judd-Ofelt spectral analysis was carried out to determine the local structure and bonding in the vicinity of rare-earth ions. The experimental oscillator strengths calculated from the absorption spectra were used to evaluate the Judd-Ofelt intensity parameters Ω_λ (λ = 2, 4 and 6). Changes in the glass density, refractive index and the values of Ω_4 and Ω_6 with different rare-earth concentrations are ascribed to changes in the glass network structure. Our results indicate that the present glass is a quite good matrix for Erbium ions, and the quantum efficiency of the 1540 nm emission was high. No quenching mechanisms were detected up to 2% of Erbium concentration.

Keywords: glass, erbium, luminescence, Judd-Ofelt parameters.

1. Introduction

Phosphate glasses are well known vitreous formers because of their high vitrification capacity and high ability to dissolve other glass formers and modifiers. On the other hand, glasses that only use phosphate as a former have low chemical durability and thermo-mechanical limitations [1]. Recent studies have demonstrated that the mechanical and thermo-mechanical properties of phosphate glasses can be improved by doping with SiO_2 without degrading the spectroscopic properties significantly [2, 3, 4]. Literature presents silicate in higher concentrations as a vitreous former which elevates the necessary annealing time and fusion temperature. In this study a fixed amount of SiO_2 is considered, enough to obtain desired chemical and mechanical resistance and preserve usual characteristics of phosphate glasses such as low melting point. Further modifications into the glass network are explained in section 3.

Among Rare Earth ions, Erbium has been extensively investigated for applications in optical fibers and amplifiers, due to the Er^{3+} $^4I_{13/2} \rightarrow {}^4I_{15/2}$ transition around 1.5 μm, that coincides with the low-loss window of standard optical communications fibers [3, 5, 6, 7, 8, 9]. The purpose of the present study was to propose a new phosphate glass combining properties of

*Corresponding author. E-mail: zamadaludwig@gmail.com

several modifiers to optimize the host matrix to receive the Rare Earth making feasible an application as mentioned above and to investigate the optical properties of Er^{3+} doped phosphate glass with composition $(40 - x)P_2O_5$-$(3 - x)SiO_2$-$(13 - x)CaO$-$(13 - x)MgO$-$(13-x)Na_2O$-$(13-x)ZnO$-$(5-x)Al_2O_3$-xEr_2O_3 with 0.3, 1.0 and 2.0 mol% concentrations. Radiative parameters, such as radiative rates, branching ratios, lifetime, quantum efficiency and quenching of the Er^{3+} $^4I_{13/2} \rightarrow {}^4I_{15/2}$ transition were determined. Influence of the Erbium concentration on the density and refractive index of the glass was also investigated.

2. Material and Methods

2.1. Glass Preparation

High quality reagents from Sigma-Aldrich were used to form the glass material. The dopant material Er_2O_3 has purity better than 99,99 %. Glass samples of the form $(40 - x)P_2O_5$-$(3 - x)SiO_2$-$(13 - x)CaO$-$(13 - x)MgO$-$(13-x)Na_2O$-$(13-x)ZnO$-$(5-x)Al_2O_3$-xEr_2O_3 with 0.3, 1.0 and 2.0 mol% were prepared using melt-quenching technique [10]. The raw materials were melted in an alumina crucible in an air atmosphere for 4h at $1200 - 1300^0$C with a heating rate of 25 C°/min to ensure complete homogeneity. The samples were quenched in a stainless-steel plate and annealed at 50 - 100 ^{0}C below the transition temperature to remove internal stress for 2 hours then cooled inside the furnace down to room temperature. The glass samples were cut to dimensions 10x10x2 mm, finely polished and used for optical and spectroscopic measurement.

2.2. Density and Refractive Index Measurements

The density of the polish glass samples was measured at room temperature according to the Archimedes method using distilled water as the immersion liquid, as well as a scale with a precision of 0.0001g. The refractive index of the samples was measured using an Abbe refractometer (1.300-1.720 nD Mod. 2WAJ) using 1-bromonaphthalene as an adhesive coating and He-Ne laser (632.8 nm) as light source. All measurements were made at room temperature, and the refractometer was calibrated with distilled water at room temperature.

2.3. Optical Absorption and Photoluminescence

The optical absorption spectra in the UV-Vis range were recorded with a UV-2550 Shimadzu spectrometer. Spectra in the NIR range were obtained by a Multi-Purpose Analyzer with a resolution of 1nm (MPA-Bruker). The photoluminescence was performed with a semiconductor laser emitting at 980 nm. Luminescence signals were collected into a Digikrom DK480 monochromator coupled to an InGaAs detector from Electro-Optical Systems, mod. IGA-030-H Receivers (NIR). The lifetime was measured via time-resolved photoluminescence technique using a semiconductor laser emitting at 980 nm, an IGA-010-H detector and a digital oscilloscope Minipa model MO-2300 to gather the data. All measurements were made at room temperature [11].

The measured oscillator strengths and the quantum efficiency of the observed transitions were estimated by the ratio between experimental and calculated lifetimes. The *Judd Ofelt* parameters Ω_2, Ω_4 and Ω_6 were determined. It is well established that Ω_6 is more affected by changes in the radial integrals $\langle 4f|r^k|5d\rangle$, than Ω_4 and Ω_2. Therefore, Ω_6 is more sensitive to changes

in the electron density of the 4f and 5d orbitals. Otherwise, Ω_2 is more affected by the asymmetry of the crystal field and by changes of the energy difference between the $4f^N$ and $4f^{(N-1)}\,5d^1$ configuration [12].

3. Results and Discussion

3.1. Structure, Density and Refractive Index Results

The addition of Na_2O further improves the solubility of rare earths leading to the possibility of using higher concentrations of dopant, while increasing the Al_2O_3 links in the P_2O_5 tetrahedral structural units, resulting in greater durability, transition temperature and a decrease of the thermal expansion coefficient [13]. The structure of phosphate glass systems based on P_2O_5 is very similar to silicate network and the models are based on PO_4 tetrahedral formed at high temperature (≈ Tg) during the initial phase of the quenching of the melt.

Figure 1 shows a schematic illustration of the non-bridging oxygen (NBO^-) formation mechanism during the melt quenching process, while the reaction temperature crosses the transition temperature (Tg) region. In this case, phosphate glass matrix is formed in the presence of Na_2O glass modifier. It can be seen that bridging oxygen (BO) bond between two adjacent PO_4 tetrahedrons are broken. The result of the reaction is a pair of NBO^-s, charge-compensated by the Na+ ions. The model assumes that the reaction can be eventually reversed, recovering the Na_2O molecule and leaving a mutually charge compensated pair of a positive vacancy oxygen (VO^+) and a negatively charged NBO^-. During the cooling of the melting and the beginning of the formation of the matrix there is a competition between the bonds being formed and eventually some silicon atoms can participate in some bonds, guaranteeing the improvement in the hardness of these glasses.

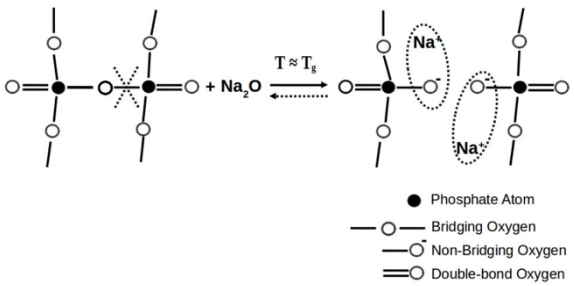

Figure 1: Schematic representation of the local phosphate glass structure being formed during the quenching process of the melt, showing the bridging oxygen (BO) bond breaking due to thermal collisions, at a T_g temperature, with the Na_2O molecule yielding a pair of charge-compensated non-bridging oxygen (NBO^-).

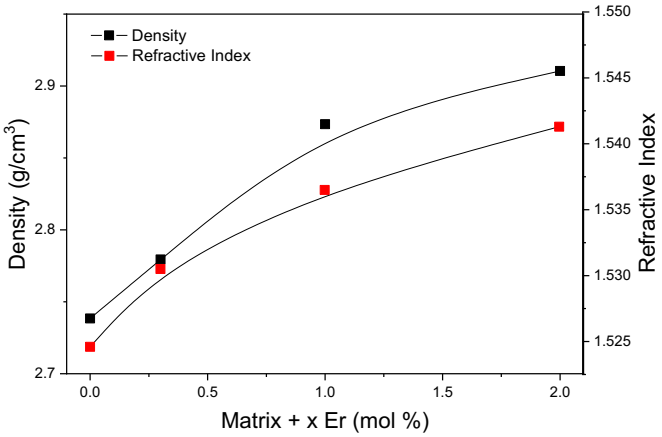

Figure 2: Density and refractive index as a function of the erbium concentration for all samples.

Figure 2 shows the density and refractive index of Er^{3+} ion in the present silicate phosphate glass system as a function of Er_2O_3 concentration. The density increases as Er_2O_3 is added to the mixture because P_2O_5 is replaced by Er_2O_3 in the glass network and Er_2O_3 which has higher density (about 3.5 times). The refractive index increases as the density increases. Similar results for the increasing of Er_2O_3 concentration were also

obtained by Rao et al [14] in their Er^{3+} co-doped Nd^{3+} magnesium lead borosilicate glasses.

3.2. Absorption Results

Figure 3 shows the room temperature UV-Vis absorption spectra of 0.3, 1.0 and 2.0 mol % of Er3+ doped phosphor-silicate glasses. The absorption spectra were recorded in the range from 200 to 850 nm and the bands that correspond to Er^{3+} transitions were identified. Twelve absorption bands are clearly observed at the UV-Vis region and correspond to the transitions from $^4I_{15/2}$ ground state level to excited states levels ($^4D_{7/2}$, $^2G_{7/2}$, $^4G_{9/2}$, $^4G_{11/2}$, $^2G_{9/2}$, $^4F_{3/4}$, $^4F_{5/2}$, $^4F_{7/2}$, $^4F_{9/2}$, $^2H_{11/2}$, $^4S_{3/2}$, $^4I_{9/2}$) located at around 39138, 28050, 27434, 26525, 24600, 22598, 22197, 20512, 19230, 18365, 15372, 12507 cm^{-1}. Additionally, two bands were observed at near infrared region at 10206 and 6515 cm^{-1}, attributed to the $^4I_{11/2} \rightarrow {}^4I_{15/2}$ and $^4I_{15/2} \rightarrow {}^4I_{13/2}$. The occurrence of all these peaks is in agreement with other findings [15, 16, 17]. Most of these transitions were observed by Assadi in their spectroscopic study of erbium doped aluminosilicate glasses. The emission due to the $^4I_{15/2} \rightarrow {}^4D_{7/2}$ transition was also detected at at 39138 cm^{-1} with medium intensity. Spectral broadening of the energy levels may be induced the two main effects: phonon broadening and electronic perturbation. Spectral substructure will probably become evident due to Stark splitting i.e. any degeneracy in the energy level structure will be removed due to the influence of interatomic electric fields. It should be noted that in an amorphous matrix such as silicate glass, the local electric fields will have a non-uniform distribution and spatial variations throughout the bulk of the sample can occur [18].

The doping levels used when manufacturing novel optical glasses are critical to the performance of the envisaged devices. The efficiency of devices such as lasers and amplifiers depend on effects such as concentration quenching.

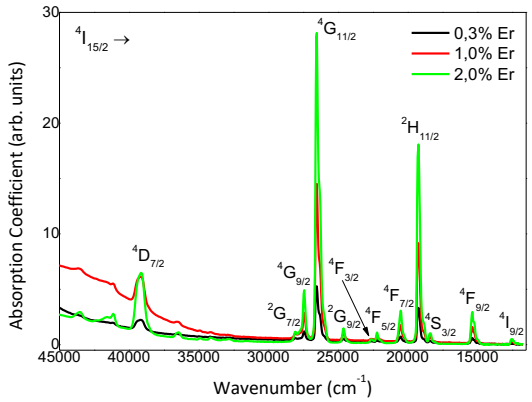

Figure 3: Optical absorption spectra of Er^{3+} ion in phosphate glass system in UV-Vis.

This is essentially a problem of cross-relaxation of the excited state energy levels induced by the close proximity of the dopant atoms to each other. This concentration quenching reduces the probability of achieving population inversion. Also, if the dopant concentration is too high, crystallization within the glass matrix can occur, dramatically increasing optical losses within the material [2].

The NIR absorption spectra for all samples are shown in Figure 4, where the absorption peaks due to $^4I_{15/2} \rightarrow {}^4I_{11/2}$ and $^4I_{15/2} \rightarrow {}^4I_{13/2}$ are exhibited [15]. The intra 4f transitions of Er^{3+} ions from $^4I_{13/2} \rightarrow {}^4I_{15/2}$ transition centered at around 1530 nm, are very important for optical devices and are strongly dependent on the concentration of Er^{3+} ions [19]. For instance, the performance of glass lasers can be altered by controlling the radiative and non-radiative decay rates of rare earth ions on the host.

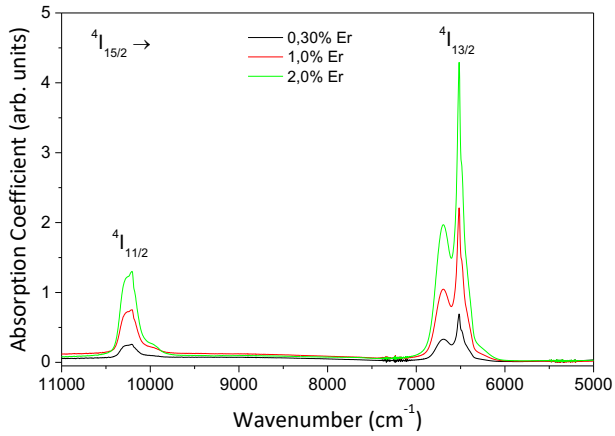

Figure 4: Optical absorption spectra of Er^{3+} ion in phosphate glass system in NIR spectra.

3.3. Photoluminescence (PL) Results

Figure 5 displays the PL spectra excited at 980 nm, with different concentrations of Er^{3+} ion in the present phosphosilicate glass system. The figure also shows that the emission of Er^{+3} is centered at 6515 cm^{-1} and increases with concentration, but this effect is not linear. The PL emission was obtained exciting defects in glassy host, that form a continuum of states [11] and also by the absorption $^4I_{15/2} \rightarrow {}^4I_{9/2}$.

In the later case, there is a nonradiative decay from the $^4I_{11/2}$ to the $^4I_{13/2}$ with further emission from the $^4I_{13/2}$ to the fundamental state $^4I_{15/2}$. The broad emission corresponds to the splitting of the electronic transition $^4I_{13/2} \rightarrow {}^4I_{15/2}$ due to the breaking of the degeneracy. Figure 6 shows the lifetime of the $^4I_{13/2} \rightarrow {}^4I_{15/2}$ Er^{3+} transition, excited at 980 nm. This decay is purely exponential. The most important feature to be pointed out is that the sample with lower Er^{3+} content presents the higher lifetime. It is also possible to note that the lifetime diminishes with the increase of the concentration of Er and therefore indicates that there are energy transfer processes taking place. Long lifetime allows high population inversion which is an important characteristic for laser application [11].

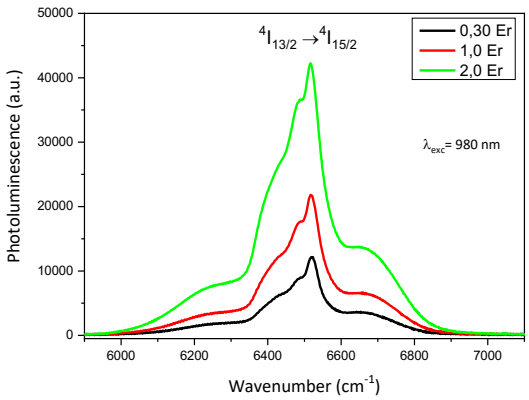

Figure 5: Near-infrared luminescence of the phosphosilicate glasses doped with Er_2O_3 (mol %).

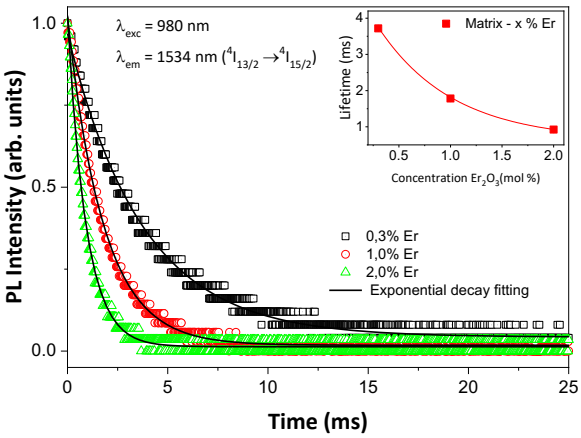

Figure 6: Photoluminescence decay of the matrix glass doped with Er_2O_3 (mol %) in the phosphosilicate glasses.

3.4. Judd-Ofelt Parameters, Lifetime and Quantum Efficiency

Using the experimental and theoretical equations of the electromagnetic dipole, oscillator strengths and different bands corresponding to the excited levels ($^4D_{7/2}$, $^2G_{7/2}$, $^4G_{9/2}$, $^4G_{11/2}$, $^2G_{9/2}$, $^4F_{3/4}$, $^4F_{5/2}$, $^4F_{7/2}$, $^4F_{9/2}$, $^2H_{11/2}$, $^4S_{3/2}$, $^4I_{9/2}$), the Judd-Ofelt parameters were obtained using the least squares

method [20 - 30]. The set of Judd-Ofelt parameters of rare earth ions in a host becomes of particular importance, since the line strength S and the branching radio β of a transition from the state $|\alpha J>$ to $|\beta J>$ are determined with the reduced matrix elements of unit tensor operator $U^{(t)}$ [31].

The Judd-Ofelt parameters have been obtained from absorption bands and the reduced matrix elements [30]. A measure of the accuracy of the fitted values of these parameters was given by root-mean-square (RMS) deviation. The results of the intensity calculations are shown in Table 1, as well as the RMS.

The determination of the Judd-Ofelt intensity parameters of Er^{3+} ions is important for the understanding of the relationship between the glassy host and the Er^{3+} emission properties [3]. These parameters were used to predict the radiative lifetimes (τ_{cal}) for the $^4I_{13/2}$ level of Er^{3+} ions. It can also be noted that both experimental and theoretical lifetime increased but the efficiency diminished. It is well known that Judd-Ofelt parameters can be related to the local structure and bonding in the vicinity of rare earth ions. We observed that Ω_2, Ω_4 and Ω_6 have similar behavior as a function of Er^{3+} concentration and follow the trend $\Omega_2 > \Omega_4 > \Omega_6$. The density and refractive index of the present glass change due to the modification of the glass network structure.

Accordingly, the values of Ω_4 and Ω_6 change with different rare-earth concentration. On the other hand, Ω_2 is related to the symmetry of the glassy hosts while Ω_6 decreases with the increase of the covalence nature of the Er − O bond [32]. The higher value of Ω_2 representing less ionic nature of chemical bond with the ligands is responsible for the increase in the covalent character [33, 34]. The smaller Ω_4 and larger Ω_6 are favorable for the luminescent transition [15, 38]. Previous observations suggest that both covalency and site selectivity of rare-earths with non-center symmetric potential contribute significantly to Ω_2, while Ω_4 and Ω_6 are mostly dependent on bulk properties such as viscosity and dielectric constant of the medium [31, 32, 33, 34, 38]. Also, Ω_2 is strongly dependent on the hypersensitive transitions, which are related to the covalency through nephelauxetic effect and affects the polarizability of the ligands around the rare earth ions. Higher ligand polarizability results in a larger overlap between rare earth ions and the ligands orbitals, i.e., a higher degree of covalency between the rare earth ion and the ligands. Thus, the increment of rare earth concentration (with reduction of Al^{3+} content) decreases the Ω_2 and the degree of covalency [27, 39]. Because Ω_6 is more dependent on changes in the electron density of the 4f and 5d orbitals, it is affected by the covalency in a different way with respect to Ω_2. Thus, Ω_6 decreases with increasing covalency between ligands and rare earth ions due to increasing electron donation of the ligands, whereas Ω_2 increases due to decreasing energy difference between the configurations. In glasses with phosphate groups, there is an additional influence on the Ω_6 parameter [27]. In the phosphate groups, one π-bond between the 3d orbital of phosphorus and the 2p orbital of a non-bridging oxygen occurs in addition to the 4 σ-bonds of the PO_4 tetrahedra [28]. If there are more than one non-bridging-oxygen in a PO_4 tetrahedron, the π-bond is delocalized over all non-bridging-oxygens within the one PO_4 tetrahedron. In the samples, Ω_2 increases with increasing phosphate content. The same tendency was found in Er^{3+} doped glasses by Zemon [40] and Zou [25].

Table 1 shows a comparison of the Judd Ofelt parameters and radiative properties (lifetime τ, quantum efficiency η) for the present samples with

other values reported in the literature. Similar lifetime and quantum efficiency were found for a phosphate matrix doped with 0.5 mol of erbium in the work of Langar et al [37]. An analysis with low (0.05, 0.1 and 0.15 mol %) erbium concentration was done by Sdiri et. al. [36] in a phosphate-borate matrix and an increase in the quantum efficiency was obtained with the increase of the erbium concentration from 0.05 to 0.15 mol %. In a sodium phosphate matrix a larger quantum efficiency was obtained with 0.5 mol % of Erbium by Hraiech et al [35] as show in Table 1

Table 1: Values of Judd-Ofelt intensity parameters (Ω_t), of the present phosphate glasses doped with Er_2O_3 (mol%), calculated (τ_{cal}) and experimental (τ_{exp}) lifetime and quantum efficiency (η) of the $^4I_{13/2}$ emission level of Er^{3+}.

1- $45P_2O_5$-$3SiO_2$-$12CaO$-$12MgO$-$12Na_2O$-$12ZnO$-$4Al_2O_3$-xEr_2O_3 with $0.3 \leq x \leq 2.0$ mol%.

2- $(46-x/2)P_2O_5$-$(46-x/2)Na_2O$-$8B_2O_3$-xEr_2O_3 with 0.5, 1.0 e 1.5mol%.

3- $85P_2O_5$–$10B_2O_3$–$(5-x)Na_2O$–xEr_2O_3 with 0.05, 0.1 and 0.15mol %.

4- $(75- x)NaH_{21}PO_4$–$20ZnO$–$5Li_2CO_3$–xEr_2O_3 (x = 0.5 mol%).

Sample	Er (mol%)	Ω_2 (10^{-20} cm^2)	Ω_4 (10^{-20} cm^2)	Ω_6 (10^{-20} cm^2)	τ_{rad} (ms)	τ_{exp} (ms)	η(%)	Ref.
1	0.3	6.43	1.84	1.33	7.16	3.72	52	This
	1.0	5.43	1.62	1.16	7.69	1.78	23	work
	2.0	5.44	1.66	1.14	7.79	0.92	12	
2	0.5	5.64	2.38	1.55	6.61	4.48	68	[32]
	1.0	4.38	2.29	1.35	7.32	3.50	48	
	1.5	7.98	2.59	2.52	4.60	1.52	33	
3	0.05	1.400	2.022	4.936	-	0.614	24	[33]
	0.1	1.283	2.501	6.237	-	0.780	37	
	0.15	5.143	3.584	7.552	-	0.884	51	
4	0.5	3.91	1.97	2.57	7.53	3.95	52	[34]
Sample	Er (mol%)	Ω_2 (10^{-20} cm^2)	Ω_4 (10^{-20} cm^2)	Ω_6 (10^{-20} cm^2)	τ_{rad} (ms)	τ_{exp} (ms)	η(%)	Ref.
1	0.3	6.43	1.84	1.33	7.16	3.72	52	This
	1.0	5.43	1.62	1.16	7.69	1.78	23	work
	2.0	5.44	1.66	1.14	7.79	0.92	12	
2	0.5	5.64	2.38	1.55	6.61	4.48	68	[32]
	1.0	4.38	2.29	1.35	7.32	3.50	48	
	1.5	7.98	2.59	2.52	4.60	1.52	33	
3	0.05	1.400	2.022	4.936	-	0.614	24	[33]
	0.1	1.283	2.501	6.237	-	0.780	37	
	0.15	5.143	3.584	7.552	-	0.884	51	
4	0.5	3.91	1.97	2.57	7.53	3.95	52	[34]

4. Conclusions

Glasses containing Er^{3+} ions have been prepared by melt technique and their optical properties were studied. It was demonstrated the high UV transmittance of the glass. The samples produced are not hygroscopic which is a huge gain compared to usual phosphate glasses. The Judd-Ofelt parameters, radiative lifetime and quantum efficiency have been determined in order to evaluate the potential of Er^{3+} ions in new phosphate glass. Decay curves for the $^4I_{13/2} \rightarrow {}^4I_{15/2}$ transition exhibits single exponential nature for all the concentration and the experimental lifetime leads to a decreasing of 3.78 to 0.92 ms with the increasing of the erbium concentration.

From the PL measurements, lifetimes and the quantum efficiencies increase with the decreasing of erbium concentration. Our findings may be useful for the development of functional glasses with good mechanical stability and at the same

time with high UV transmittance and optical properties.

Acknowledgments

This work was supported by FAPEMIG, CNPq and CAPES. FAPEMIG (APQ-01615-12 and APQ-01586-10).

References and Notes

[1] E. S. H. Nandyala, Current Trends on Lanthanide Glasses and Materials: Materials Research Foundations Volume 8, Materials Research Forum, USA, 2017.

[2] J. Y. Hu, H. W. Yang, Y. J. Chen, J. S. Lin, C. H. Lai, Y. M. Lee, T. Zhang, Properties and structure of Yb^{3+} doped zinc aluminum silicate phosphate glasses, J. Non-Cryst. Solids 357 (2011) 2246–2250.

[3] Y. K. Chen, L. Wen, L. L. Hu, W. Chen, Y. Guyot, G. Boulon, Raman and optical absorption spectroscopic investigation of Yb–Er codoped phosphate glasses containing SiO2, Chin. Opt. Lett. 7 (2009) 56–59.

[4] P. Wang, C. Wang, L. L. Hu, L. Y. Zhang, Effect of SiO_2 on the Stark splitting enlargement of Yb^{3+} in phosphate glass, Acta Phys. Sin. 5 (2006) 311–317.

[5] P. Nandy, G. Jose, Erbium doped phospho-tellurite glasses for 1.5 mm optical amplifiers, Opt. Comm. 265 (2) (2006) 588–593.

[6] E. O. Serqueira, R. F. de Morais, V. Anjos, M. J. V. Bell, N. O. Dantas, Effect of Na2O concentration on the lifetime of Er^{3+} -doped sodium silicate glass, RSC Advances 3 (46) (2013) 24298–24306.

[7] A. P. Carmo, M. J. V. Bell, Z. D. Costa, V. Anjos, L. Barbosa, E. Chillcce, J. M. Giehl, W. M. Pontuschka, Optical and spectroscopic properties of soda lime alumino-silicate glasses doped with erbium and silver, Opt. Mater. 33 (12) (2011) 1995–1998.

[8] M. J. Weber, T. E. Varitimos, B. H. Matsinger, Optical intensities of rare-earth ions in yttrium orthoaluminate, Phys. Rev B 8 (1) (1973) 47–53.

[9] G. Jia, C. Tu, J. Li, Z. You, Z. Zhu, B. Wu, Crystal structure, Judd-Ofelt analysis, and spectroscopic assessment of a $TmAl_3(BO_3)_4$ crystal as a new potential diode-pumped laser near 1.9 mm, Inorg. Chem. 45 (2006) 9326–9331.

[10] D. T. Bowron, A study of rare earth doped silicate and phosphate glasses, doctor of philosophy (phd) thesis, university of Kent.

[11] A. S. Pinheiro, A. M. Freitas, G. H. Silva, M. J. V. Bell, V. Anjos, A. P. Carmo, N. O. Dantas, Laser performance parameters of Yb^{3+} doped UV-transparent phosphate glasses, Chem. Phys. Let. 592 (2014) 164–169.

[12] N. T.Thanh, V. X. Quang, V. P. Tuyen, N. V. Tam, T. Hayakawa, B. T. Huy, Role of charge transfer state and host matrix in Eu^{3+} doped alkali and earth alkali fluoro-aluminoborate glasses, Opt. Mat. 34 (2012) 1477–1481.

[13] S. V. G. V. A. Prasad, M. S. Reddy, N. Veeraiah, Nickel ion - a structural probe in $BaO - Al_2O_3 - P_2O_5$ glass system by means of dielectric, spectroscopic and magnetic studies, Journal of Physics and Chemistry of Solids 67 (2006) 2478–2488.

[14] T. G. V. M. Rao, A. R. Kumar, K. Neeraja, N. Veeraiah, M. R. Reddy, Optical and structural investigation of Eu^{3+} ions in Nd^{3+} co-doped magnesium lead borosilicate glasses, Journal of Alloys and Compounds 557 (2013) 209–217.

[15] E. S. Sazali, R. Sahar, S. K. Ghoshal, S. Rohani, R. Arifin, Judd-Ofelt intensity parameters of erbium doped lead tellurite glass, J. Non-Oxide Glasses 6 (4) (2014) 61–67.

[16] A. A. Assadi, A. Herrmann, R. Lachheb, C. R. K. Damak, R. Maâlej, Experimental and theoretical spectroscopic study of erbium doped aluminosilicate glasses, J. Lumin. 176 (2016) 212– 219.

[17] G. Devarajulu, O. Ravi, C. M. Reddy, S. Z. A. Ahamed, B. D. P. Raju, Spectroscopic properties and upconversion studies of Er^{3+}-doped SiO_2-Al_2O_3-Na_2CO_3-SrF_2-CaF_2 oxyfluoride glasses for optical amplifier applications, J. Lumin. 194 (2018) 499–506.

[18] M. T. Rinke, H. Eckert, The mixed network former effect in glasses: solid state NMR and XPS structural studies of the glass system (Na_2O) x $(BPO_4)1 – x$, Phys. Chem. Chem. Phys. 13 (2011) 6552–6565.

[19] A. A. Reddy, S. S. Babu, G. V. Prakash, Er^{3+} doped phosphate glasses with improved gain characteristics for broadband optical amplifiers, Opt. Comm 285 (2012) 5364–5367. 17

[20] B. R. Judd, Optical absorption intensities of rare-earth ions, Phys. Rev. 127 (3) (1962) 720–761.

[21] G. S. Ofelt, Intensities of crystal spectra of rare-earth ions, J. Chem. Phys. 37 (3) (1962) 511–520.

[22] P. Nachimuthu, R. Jagannathan, Judd-Ofelt parameters, hypersensitivity, and emission characteristics of Ln^{3+}(Nd^{3+}, Ho^{3+}, and Er^{3+}) ions doped in $PbO–PbF_2$ glasses, J. Am. Ceram. Soc. 82 (1999) 387–392.

[23] R. Reisfield, C. Jorgensen, Lasers and Excited States of Rare-earths, Springer-Verlag, NY, 1977.

[24] G. F. Yang, D. M. Shi, Q. Y. Zhang, Z. H. Jiang, Spectroscopic properties of Er^{3+}/Yb^{3+} codoped PbO glasses, J. Fluorescence 18 (2008) 131–137.

[25] X. Zou, T. Izumitami, Spectroscopic properties and mechanisms of excited state absorption and energy transfer upconversion for Er^{3+} doped glasses, J. Non-Cryst Solids 162 (1993) 68–80.

[26] K. Pradeesh, C. J. Oton, V. K. Agotiya, M. Raghavendra, G. V. Prakash, Optical properties of Er^{3+} doped alkali chlorophosphate glasses for optical amplifiers, Opt. Mater. 31 (2008) 155–160.

[27] S. Tanabe, T. Ohyagi, N. Soga, T. Hanada, Compositional dependence of Judd-Ofelt parameters of Er^{3+} ions in alkali-metal borate glasses, Phys. Rev. B 46 (1992) 3305–3310.

[28] A. A. Reddy, S. S. Babu, K. Pradeesh, C. J. Otton, G. V. Prakash, Optical properties of highly Er^{3+} -doped sodium-aluminium-phosphate glasses for broadband 1.5 μm emission, Journal of Alloys and Compounds 509 (2011) 4047–4052.

[29] G. A. Kumar, R. E. Riman, L. A. D. Torres, S. Banerjee, M. D. Romanelli, T. J. Emge, J. G. Brennan, Near-infrared optical characteristics of chalcogenide-bound Nd^{3+} molecules and clusters, Chem. Mater. 19 (2007) 2937–2946.

[30] G. V. Prakash, S. S. Babu, A. A. Reddy, Optical Amplifiers from Rare-Earth Co-Doped Glass Waveguides, Edited by Paul Urquhart, 2011.

[31] S. Tanabe, T. Hanada, T. Ohyagi, N. Soga, Correlation between ^{151}Eu Mossbauer isomer shift and Judd-Ofelt Ω_6 parameters of Nd^{3+} ions in phosphate and silicate laser glasses, Phys. Rev. B 48 (14) (1993) 10591–10594.

[32] V. V. Kumar, K. A. Bhatnagar, R. Jagannathan, Structural and optical studies of Pr^{3+}, Nd^{3+}, Er^{3+} and Eu^{3+} ions in tellurite based oxyfluoride, TeO_2-LiF, glass, J. Phys. D: Appl. Phys. 34 (2001) 1563–1568.

[33] C. K. Jorgensen, R. Reisfeld, Judd-Ofelt parameters and chemical bonding, J. Less-Common Mat. 93 (1) (1983) 107–112.

[34] P. Subbalakshmi, N. Veeraiah, Optical absorption and fluorescence properties of Er^{3+} ion in MO - WO_3 - P_2O_5 glasses, J Phys. and Chem. Sol. 64 (2003) 1027–1035. [38] S. D. Emami, A. Zarifi, H. A. A. Rashid, A. R. Muhammad, M. C. Paul, A. Halder, S. K. Bhadra, H. Ahmad, S. W. Harun, Gain-shift induced by dopant concentration ratio in a thulium-bismuth doped fiber amplifier, Opt. Exp. 22 (6) (2014) 7075–7086.

[35] S. Hraiech, C. Bouzidi, M. Férid, Luminescence properties of Er^{3+} -doped phosphate glasses, Physica B: Condensed Matter 522 (2017) 15–21.

[36] N. Sdiri, H. Elhouiche, C. Barthou, M. Ferid, Spectroscopic properties of Er^{+3} and Yb^{+3} doped phosphate–borate glasses, Journal of Molecular Structure 1010 (2012) 85–990.

[37] A. Langar, C. Bouzidi, H. Elhouichet, M. Férid, Er-Yb codoped phosphate glasses with improved gain characteristics for an efficient 1.55 μm broadband optical amplifiers, Journal of Luminescence 148 18 (2014) 249–255.

[38] H. Desirena, E. D. Rosa, L. A. Diaz-Torres, G. A. Kumar, Concentration effect of Er^{3+} ion on the spectroscopic properties of Er^{3+} and Yb^{3+}/Er^{3+} co-doped phosphate glasses, Opt. Mater. 28 (5) (2006) 560–568.

[39] I. Jlassi, H. Elhouichet, S. Hraiech, M. Ferid, Effect of heat treatment on the structural and optical properties of tellurite glasses doped erbium, J. Lum. 132 (2012) 832–840.

[40] S. Zemon, G. Lambert, L. J. Andrews, W. J. Miniscalco, B. T. Hall, T. Wei, R. C. Folweiler, Characterization of Er^{3+} doped glasses by fluorescence line narrowing, J. Appl. Phys. 66 (1991) 6799–6811.